AVIRIS Measurements of Chlorophyll, Suspended Minerals, Dissolved Organic Carbon, and Turbidity in the Neuse River, North Carolina

Mark A. Karaska, Robert L. Huguenin, Jeff L. Beacham, Mo-Hwa Wang, John R. Jensen, and Ronald S. Kaufmann

Abstract

Many aquatic ecosystems in the United States and worldwide are impaired by the over-enrichment of waters by nutrients. In advanced stages, the process of eutrophication can cause harmful algae blooms. This research retrieved the concentrations of suspended chlorophyll (Chl), suspended minerals (SM), colored dissolved organic carbon (DOC), and turbidity (total attenuation) from AVIRIS imagery of a severely over-enriched waterway in North Carolina, and evaluated if these parameters could be used as indicators of conditions leading to algae blooms. A digital image processing algorithm called QSC1 (Quantitative Shoreline Characterization, Version 1.0) was used. The retrieved water quality parameter values were tested by statistical comparisons to field measurements made at the time of the AVIRIS data collection. Applying QSC1 to AVIRIS imagery resulted in measurements of Chl that correlated well with field measurements (r = 0.84). Problems with field sampling prevented the assessment of retrieved SM and DOC. The statistical correlation analysis indicated that, for comparison to remotely sensed data, field measurements in the steadily flowing Neuse River must be collected within two hours of the imagery. Thematic maps of each water quality parameter were generated from the imagery and evaluated. The maps of Chl showed spatial patterns consistent with the field data and circulation of the river, and indicated potential point and non-point sources. Statistical and principle component analyses were used to assess whether the AVIRIS water quality measurements were directly or indirectly related to parameters and conditions indicative of nutrient loading and algae blooms that were measured in the field. The AVIRIS measurements were used to create a new index of eutrophication, the Algae Production Potential Index (APPI), for the purpose of mapping where conditions of high nutrient loading and potential algae blooms exist. The index uses direct measurements of Chl, DOC, and SM (as a surrogate for phosphate). These measurements are combined in a GIS model based on ecological relationships. Although not field verified, the APPI map shows patterns of algae bloom conditions that are similar in size, scale, and location to previous blooms in the Neuse.

M.A. Karaska, R.L. Huguenin, and M.-H. Wang are with Applied Analysis Inc., 630 Boston Road, Billerica, MA 01821 (mkaraska@discover-aai.com).

J.L. Beacham and R.S. Kaufmann are with Earth Tech, 10 Patewood Dr., Bldg. 6, Ste. 500, Greenville, SC 29615.

J.R. Jensen is with the Department of Geography, University of South Carolina, Columbia, SC 29208.

Introduction

The 1996 National Water Quality Inventory states that 40 percent of impaired rivers, 51 percent of impaired lakes, and 57 percent of impaired estuaries in the U.S. are affected by eutrophication that can result in algae formation which kills fish, endangers human health, and impacts local economic, municipal, and recreational use of the water (EPA, 1996). Nitrogen and phosphorous are the primary nutrients responsible for the algae blooms.

The primary objective of this research was to measure how accurately turbidity and the concentrations of chlorophyll (Chl), suspended minerals (SM), and dissolved organic carbon (DOC) could be measured using remotely sensed data obtained by the Advanced Visible Infrared Imaging Spectrometer (AVIRIS). This research first established a baseline accuracy using three TM-equivalent AVIRIS bands (created by combining AVIRIS bands), necessary for determining the advantages of hyperspectral over multispectral data (a goal of NASA's Hyperspectral EOCAP). These parameters were evaluated because they are the dominant constituents affecting the spectral reflectance of water (Bukata *et al.*, 1995; Huguenin *et al.*, 2004). Water quality digital image processing software called QSC1 was used to process the AVIRIS imagery (Huguenin *et al.*, 2004). The remote sensing derived parameters were evaluated by statistical comparisons to field measurements that were collected close to the time of the AVIRIS collection.

The ability to accurately monitor and map nutrient loading over large expanses of surface water and identify early warning signs of algae blooms could provide a predictive planning and impact analysis tool for water resource managers. This information is valuable to industries discharging into the river basin; fisheries and recreational industries; municipal planning agencies; federal, state, and local environmental agencies; and the Environmental Protection Agency. Therefore, a secondary objective was to assess if the AVIRIS-derived water quality measurements were directly or indirectly related to parameters and conditions indicative of nutrient loading and algae blooms. The goal was to use these remote measurements as direct indicators or surrogate measures of nutrient loading and/or conditions leading to toxic algae blooms.

The approach was to (1) acquire AVIRIS imagery of the Neuse River in North Carolina and near-coincident *in situ*

Photogrammetric Engineering & Remote Sensing
Vol. 70, No. 1, January 2004, pp. 125–133.

0099-1112/04/7001–0125/$3.00/0

water quality measurements; (2) process the imagery to retrieve turbidity and concentrations of Chl, SM, and DOC; (3) statistically measure the correlation of AVIRIS-derived Chl, SM, DOC, and turbidity measurements to field measurements; and (4) develop models to map conditions leading to harmful algae blooms, identifying links between Chl, SM, DOC, and turbidity and other processes indicative of algae blooms and using Chl, SM, and DOC as surrogate measures of other parameters more indicative of algae bloom conditions.

In Situ and Remote-Sensing-Derived Water Quality Measurement

Water quality monitoring and modeling currently relies primarily on *in situ* shipboard sampling, laboratory analysis, and interpolation that are labor intensive and expensive. It is often not economically feasible or practical to sample large geographic areas using these methods. For these reasons, research has been taking place to derive measurements of water quality parameters using remote sensing techniques.

Gordon and Morel (1983) provided an early discussion of the analytical approaches for measuring concentrations of water constituents in ocean and coastal waters using remotely sensed data. Khorram and Cheshire (1985) measured and mapped salinity, chlorophyll *a*, turbidity, and total suspended solids in the Neuse River estuary with Landsat Multispectral Scanner imagery. They demonstrated that chlorophyll (r^2 = 0.70) and turbidity (r^2 = 0.76) could be measured with reasonable accuracy with this broad-band visible (a green and red band) and near-infrared (two bands) sensor. Jensen *et al.* (1989) mapped suspended sediment in Laguna de Terminos, Mexico using Landsat Thematic Mapper (TM) imagery. Ramsey and Jensen (1990) and Ramsey *et al.* (1993) used high spatial resolution aircraft multispectral scanner data to map chlorophyll *a* and turbidity in fresh water reservoirs in South Carolina. Dekker *et al.* (1994) discussed the use of remote sensing for deriving inland water quality parameters. Bukata *et al.* (1995) summarized the theoretical basis for optical remote sensing of water quality parameters. Woodruff *et al.* (1999) measured light attenuation, as a measure of turbidity, in Advanced Very High Resolution Radiometer (AVHRR) imagery of the Neuse River estuary. A general optical equation that related satellite-derived reflectance (nominally at 630 nm) to light attenuation yielded a general relationship (r^2 = 0.72) that was robust under a variety of environmental conditions. The relationship between reflectance and suspended sediment concentration was less robust. Richardson and Kruse (1999) classified three phytoplankton bloom types in Florida Bay with AVIRIS imagery. In these phytoplankton rich waters, algae is the dominant constituent and, therefore, spectral signatures of the different algae pigments could be classified with the same spectral matching techniques used for terrestrial materials (Spectral Angle Mapper in this case). In waters where the concentration of algae is lower or where SM and DOC are present to confuse the spectral response of the algae, traditional classification techniques are less accurate. Recently, Huguenin *et al.* (2004) described an automated subpixel photobathymetry and water quality mapping method used to simultaneously retrieve Chl, SM, and DOC, and derive turbidity. That process was used in this study. It is described further below.

Study Area and Methodology

Neuse River Study Area

The Neuse River drains part of the central North Carolina Piedmont and flows east into Pamlico Sound. It was selected as a study site because it experiences extensive nutrient loading (primarily nitrogen and phosphate) from agricultural runoff, sewage discharge, increased urbanization, and ground water and atmospheric pollutant inputs (Copeland and Gray, 1989; Paerl *et al.*, 1995). These excess nutrients cause frequent algae blooms and occasional fish kills, which create human health hazards and impact the local economic, municipal, and recreational use of the water. Nutrient loading increases during the high-flow, winter-spring periods, with periodic pulses due to rain events (Paerl *et al.*, 1998; Pinckney *et al.*, 1988). The factors causing light attenuation (organic matter, phytoplankton, and suspended sediments) vary temporally as well as spatially (Woodruff, 1999). A 110-km-long segment of the Neuse River from the mouth in Pamlico Sound to its narrow channel west of New Bern, North Carolina was studied. The majority of this segment contains the estuary where the river is one to three miles (1.6 to 4.8 km) wide, has very little influence from diurnal tides, and the circulation is strongly influenced by wind.

AVIRIS Data Collection

AVIRIS is an experimental hyperspectral sensor developed by NASA JPL (Geotz *et al.*, 1985). It contains 224 spectral bands, approximately 10 nm wide, in the 0.4- to 2.4-µm region and has 20- by 20-m spatial and 16-bit radiometric resolution. Six flightlines of AVIRIS data were collected over the Neuse River between 10:19 and 10:39 AM EST, on 20 July 1999. The skies were 90 percent cloud-free, but thin wispy clouds and haze covered about five percent of the river area. Winds were generally calm. The AVIRIS data were georegistered to 1:24,000-scale topographic maps with a root-mean-squared error (RMSE) of less than 20 m (one AVIRIS pixel).

Water Quality Retrieval Algorithm

The QSC1 subpixel photobathymetry and water quality mapping software was described in a separate paper (Huguenin *et al.*, 2004). The software utilizes subpixel processing (*Subpixel Classifier*) to explicitly compensate for the affects of the atmosphere, sun and sky reflections from the water surface, subpixel contributions from exposed land, and variations in bottom material properties. QSC1 automatically converts the detected water spectrum into units of apparent reflectance, and retrieves water depth (optional) and water composition (concentrations of suspended chlorophyll, suspended sediments, and colored dissolved organic carbon), from which clarity (vertical and horizontal subsurface sighting ranges, and turbidity) is derived on a per-pixel basis. The calculations are based on a detailed radiative transfer model, consistent with optical models and data reviewed by Bukata *et al.* (1995) and other investigators. QSC1 can measure depth, but it requires interactive user development of signatures based on *in situ* "ground reference" information. For cases where the bottom is not visible, water composition and clarity information alone can be derived, eliminating the need for depth information.

The QSC1 software requires an estimate of the general water quality characteristics of a reference set of water pixels in the image. Based on *in situ* information, the user interactively selects a "water quality category" for the water body. The choices include "Ocean," "Coastal," and five inland trophic status classes (Ultra-Oligotrophic, Oligatrophic, Mesotrophic, Eutrophic, or Hypereutrophic). Each of these categories has a standard model composition (concentrations of Chl, SM, and colored DOC) and a corresponding reference volume reflectance spectrum. The volume reflectance, $R_{vol}(n)$, for the water component of each pixel is then automatically computed. The composition for the water detection is then determined from $R_{vol}(n)$ using a three-dimensional pre-computed look-up table approach. From the derived composition, several water clarity parameters are computed for each pixel. These include Vertical and Horizontal Subsurface Sighting Ranges ($VSSR(n)$ and $HSSR(n)$, respectively), and turbidity at three wavelengths, as well as turbidity confidence values.

A primary limitation of QSC1 is that a representative water quality category is not always easy to estimate, either because it is unknown or the image may contain a diversity of water classes.[1] A second limitation is that errors due to bottom radiance are introduced in shallow waters. Consequently, the water quality results from QSC1 are strictly valid only for those pixels for which bottom radiance does not contribute.

The QSC1 algorithms use only three spectral bands in the visible range of the spectrum (the first three TM band positions) and are implemented as a module for use with ERDAS IMAGINE software. The visible wavelength range, 400 to 700 nm, is typically the dominant portion of the electromagnetic spectrum that penetrates water and thus contains information about the water column. AVIRIS contains 30 relatively narrow (10-nm) spectral bands in this range. The non-visible AVIRIS bands typically contain less water quality information because light typically does not penetrate the water to the same extent at these wavelengths. AVIRIS bands in the NIR and SWIR regions could, however, provide useful information about surface conditions and surface aquatic vegetation.

This research first evaluated the utility of three TM-equivalent AVIRIS bands (created by combining AVIRIS bands) to establish a baseline, which is necessary for determining the advantage of hyperspectral over multispectral data such as TM (a goal of NASA's Hyperspectral EOCAP). Performance of the QSC1 software with TM imagery is well tested. The TM band passes were also selected for the baseline case to enable evaluation of 12-bit versus 8-bit precision, band optimization, and other potential advantages of hyperspectral imagery over multispectral imagery. Several comparison results (e.g., optimal bandwidths and band positions) were reported in the Hyperspectral EOCAP final report (Karaska, 2002). After this baseline comparison, other three-band subsets of AVIRIS (individual bands and/or averages of bands) were evaluated in an attempt to identify the three bands from which the results most closely correlated with the field measurements. The AVIRIS data set was only processed with the QSC1 software (requiring only three input bands). AVIRIS provided an ideal data set for band selection.

QSC1 can use any combination of three bands, defined by the choice of absorption and scattering coefficient wavelengths used to populate the look-up table. The AVIRIS bands corresponding to the first three Landsat TM bands (TM1, 0.45 to 0.52 µm; TM2, 0.52 to 0.60 µm; and TM3, 0.63 to 0.69 µm) were averaged (weighted by band overlap) to produce TM-equivalent bands, but retaining the 12-bit precision. Twenty-two of the 30 AVIRIS visible bands comprised the TM-equivalent bands.

The absorption and scattering cross-sections of Chl, SM, and DOC suspended in lake water, reported by Bukata *et al.* (1995) for lake water, illustrate that these three parameters can effectively be discriminated using relatively broad band passes. Chl, SM, and DOC do not have strong narrow absorption or emission features like some minerals, but instead have broad general features. Although there may be distinct advantages for using optimally selected narrower bands, they are not required for the simultaneous retrieval of these three parameters. This is consistent with the findings of Holyer and Sandige (1996). In evaluating AVIRIS data for water depth and inherent optical properties at two Florida sites, those authors observed that the AVIRIS data had relatively low dimensionality with a high degree of spectral over-sampling; therefore, not all spectral bands were needed. It is also consistent with the findings using Ikonos multispectral imagery reported by Huguenin *et al.* (2004). The bandwidths of the first three TM or Ikonos bands were found to be adequate for discriminating these parameters. The wavelength range of the first three TM or Ikonos bands cover the majority of the light-penetrating 450- to 700-nm range.

Probably the greatest potential advantage of the hyperspectral data is in deriving additional water quality information. This may include separation of chlorophyll *a* from phaeophytin, chlorophyll *a* from *b*, detection of additional pigment materials, and possibly detection of dissolved O_2. The various chlorophyll, phaeophytin, and other pigments have distinct absorption and scattering spectra, so that they could potentially be discriminated with the additional bands. Dissolved oxygen is more problematic, because its absorption feature near 680 nm is very weak. These possibilities will be examined in future work.

In Situ Water Quality Measurements

Between the hours of 8:30 AM and 3:30 PM EST on 20 July 1999, water samples were collected at 25 surface sites (plus 28 subsurface sites) along five transects across the river. (These transects are shown in Plate 1). The transects and sample stations corresponded with the water sample stations of a state and local water sampling program called MODMON (MODMON, 2001). Water chemistry measurements included parameters

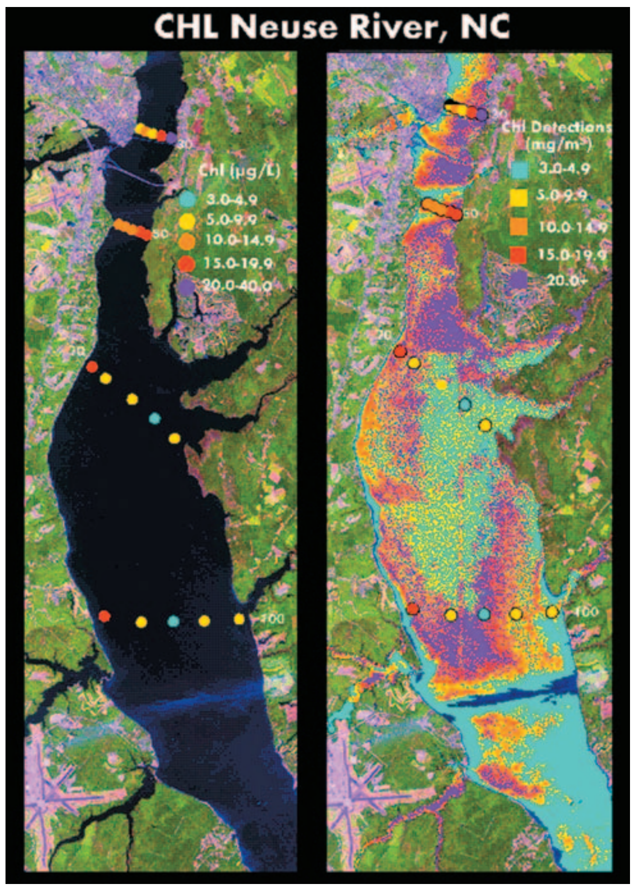

Plate 1. The chlorophyll field data overlaid on one AVIRIS image segment on the left and AVIRIS-derived Chl concentrations and field data on the right.

[1] A comprehensive evaluation of depth accuracy of the QSC1 software was carried out in 1999 by the Naval Oceanographic Office (Remote Sensing Division, Integration and Technology Department, located at Stennis Space Center, Mississippi) at the request of the Advanced MASINT Branch of the National Air Intelligence Center/DXDA (Wright Patterson Air Force Base, Ohio). The results of that independent performance evaluation are summarized in Huguenin *et al.* (2004). A newer version of the software, QSC2, is not influenced by these limitations, but it was unavailable at the time of this study.

equivalent to Chl, SM, DOC, and turbidity. In addition, the following laboratory measurements were made to further understand the geochemical and ecological processes of the river: temperature, pH, dissolved oxygen, nutrients (nitrogen and phosphorous compounds), pigments (chlorophyll), dissolved constituents (tannin, inorganic compounds), and stable isotopes of oxygen, hydrogen, and nitrogen. Although most of these parameters cannot be directly measured with AVIRIS, they are key indicators of water quality and needed to be assessed through aqueous geochemical models for linkages to parameters that might be measured with AVIRIS.

Water samples were collected less than 50 cm below the surface, 2 m below the surface, and 1 m from the bottom, at each location, by crews in three boats. The samples were kept on ice and processed in one of three laboratories depending on the analysis. The three field crews used the same instrumentation and followed the same procedures. GPS coordinates were collected at each sample location and the corresponding AVIRIS pixels at these locations were identified in the imagery. The AVIRIS image was georegistered to 1:24,000-scale topographic maps with an RMS error of less than 20 m (one AVIRIS pixel). To avoid any potential geo-positional uncertainty, a 3- by 3-pixel window of AVIRIS measurements, centered around the field GPS coordinate, was averaged for comparison to the field measurements.

Weather conditions in the Neuse River area on 20 July were ideal for algae blooms. Heavy rains created widespread surface runoff the week before, followed by several days of heavy cloud cover (during which runoff was transferred into the river), and then sunny skies for several days before the AVIRIS collection provided the energy for algae production. The state Neuse River Estuary modeling and monitoring program (MODMON, 2001) reports that algae blooms, leading to hypoxic and anoxic conditions, are a regular occurrence on sunny days in July, along these segments of the river.

Results and Discussion

Accuracy of AVIRIS Water Quality Measurements

The accuracy of the AVIRIS-derived Chl, SM, DOC, and turbidity measurements were evaluated in several ways. The spatial patterns of the four parameters were first evaluated visually. The patterns were not randomly distributed, but instead were generally consistent with expected controlling processes. Chlorophyll patterns were consistent, for example, with a wind-driven system. Chlorophyll and suspended mineral patterns were also consistent with land use in the area or point sources known to influence parameter concentrations.

The AVIRIS water quality measurements were also assessed for accuracy using ground reference water sampling data. The water samples were acquired along five transects, at times ranging from less than an hour to a little over four hours from the time of image acquisition. The parameters empirically sampled in the field were necessarily different than the parameters optically sampled by the imagery. As a result, there were uncertainties about the equivalence of field and optical parameters for the accuracy assessment. The field samples contained less than a liter of water, were collected at 0.5-m depths, and were collected over just a few meters distance. Conversely, each 20- by 20-m AVIRIS pixel sampled a 400-m^2 area to a depth of approximately a meter or more. Measurements from nine AVIRIS pixels (3,600 m^2) were averaged and compared to the field measurements. There were also potential errors in determining the exact image location corresponding to the field measurement. Significant effort was expended to reconcile the differences between the image-derived and field-derived information, and to develop a meaningful assessment of the accuracy of the processed imagery.

Observations about Water Quality Parameter Equivalence

The remote-sensing-assisted algorithms measured the concentrations of suspended chlorophyll, suspended minerals, and colored dissolved organic carbon. From these concentrations, turbidity and subsurface sighting ranges (horizontal and vertical) were calculated at three different wavelengths. These parameters were independently measured for each water pixel in the image, providing thematic maps of each of these parameters for the entire river system (including tributaries) included within the image area of coverage.

Chlorophyll

The field samples were analyzed for a much larger set of parameters. These parameters were selected not only for accuracy assessment of the processed imagery, but also for developing an aqueous geochemical model for linking the optical parameters to relevant water quality properties of the river system. Only one of the image-derived parameters could be considered "equivalent" to a field parameter: the image-derived suspended chlorophyll and sample-derived total chlorophyll concentrations.

Dissolved Organic Carbon

There was no attempt to extract the colored dissolved organic carbon (melanoid components) concentration from the field samples. The field-derived tanin and lignin concentrations represented the only direct measurement of dissolved organic carbon. The colored fulvic and humic acid components of primary interest were not included.

Suspended Mineral Concentration

There was no attempt to perform a gravimetric analysis for suspended minerals. The closest relevant field-derived measurement was the concentration of total suspended solids (TSS), which was determined by an optical measurement of absorbance at 610 nm along a 22.4-mm cell path. This includes all suspended and dissolved organic and inorganic materials that attenuate radiance at 610 nm, thereby generally providing an overestimate of the suspended minerals concentration. Beyond this, a significant problem with the TSS estimate is that suspended particles frequently settle out in the sample jar before water is drawn and placed in the TSS sample cell. Furthermore, only some of the suspended particles that make it into the sample cell remain suspended within the optical path, according to the sampling team.

Correlation of Remote-Sensing-Derived Water Quality Parameters with *In Situ* Measurements

Chlorophyll Concentrations

The field chlorophyll measurements were grouped into concentration categories, color coded, and displayed as colored dots on the AVIRIS image so that they could be visually compared to the thematic maps of these parameters generated from the hyperspectral data. For example, Plate 1 displays an AVIRIS image segment on the left with the color-coded field data overlaid. The remote-sensing-derived Chl concentration is displayed on the right. The concentration categories and color assignments are the same for the field and AVIRIS measurements (see key). It can be observed from this scene that the AVIRIS measurements of Chl correspond well with the field measurements, especially for transect 30 and 50. For example, in the "neck" region (top of image), both sets of results indicate high concentrations along the right side of the river and lower concentrations along the left. The statistical correlation between the field measurements and AVIRIS measurements of Chl are displayed in graphical form in Figure 1. Each of the five measurements, in each of five transects, are plotted. The concentrations of Chl, measured by both methods, are very similar.

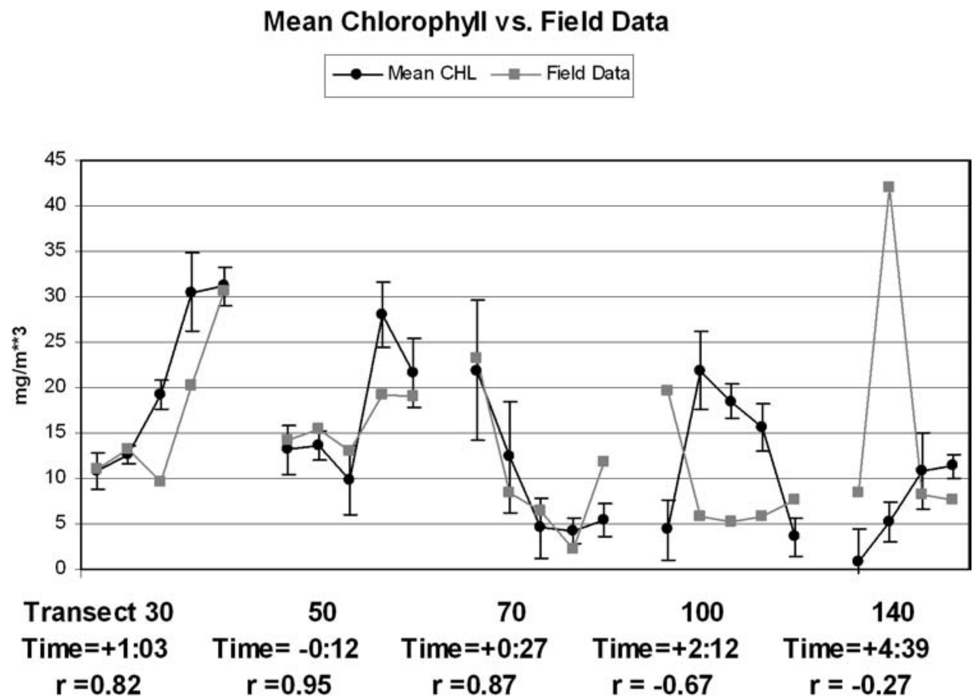

Figure 1. The comparison and statistical correlation between the *in situ* (field) chlorophyll measurements and AVIRIS-derived mean chlorophyll measurements, for the five samples in five transects. Time is the length of time after the AVIRIS imagery was collected.

The correlation coefficient (r) for each transect is also listed. For transect 50, field sampled 12 minutes before the AVIRIS overflight, the correlation coefficient is 0.95. For the three field transects measured within one hour of the AVIRIS collection (transects 30, 50, and 70), r exceeds 0.81. Transects 100 and 140 were collected more than two and four hours, respectively, after the AVIRIS collection and had the lowest correlations.

Figure 2 is a graph showing the correlation for each transect plotted against the elapsed time between the field data collection and the AVIRIS overflight. The field samples measured closest to the time of the AVIRIS collection correlate most strongly, suggesting that the flow of the river influenced the correlation results. The velocity of the river, measured at two shore locations on 20 July, was 180 m/hr. In steadily flowing or circulating water bodies, such as the Neuse River, the timing of water sampling in the field is critical for comparison to remote measurements.

The imagery revealed distinct patterns and gradients of chlorophyll concentration, and the best agreements with ground truth occurred where concentrations were most spatially uniform around the sample location along the direction of flow. Some of the field-measured concentrations agreed to

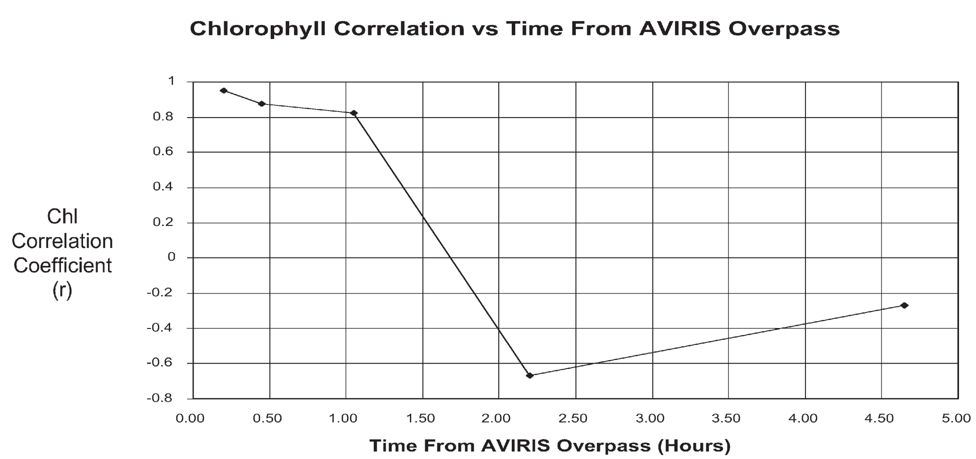

Figure 2. The chlorophyll correlation for each transect plotted versus the elapsed time between the field data and the AVIRIS collection.

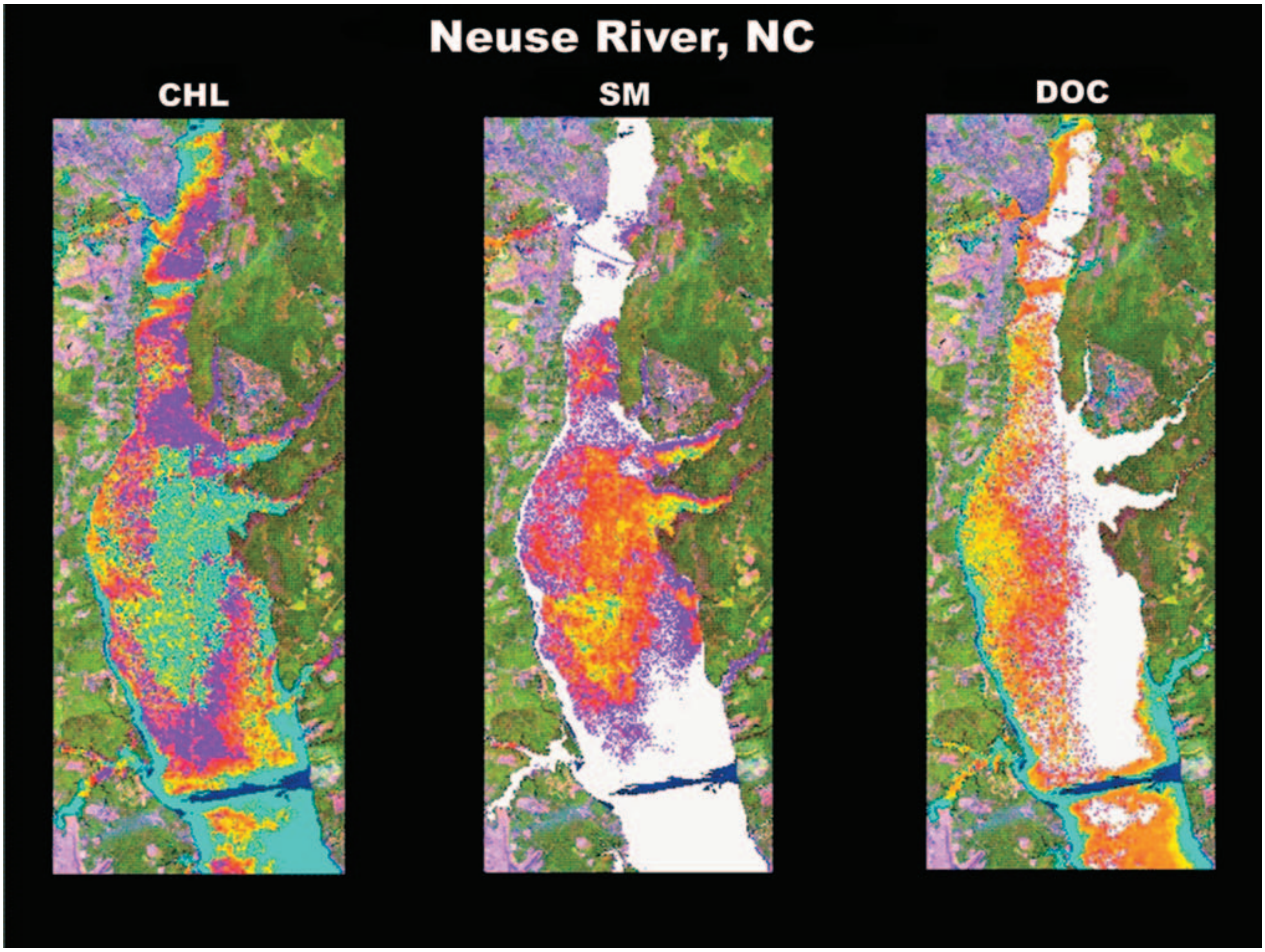

Plate 2. AVIRIS-derived thematic maps of chlorophyll, suspended minerals, and colored disolved organic carbon (northeast is up).

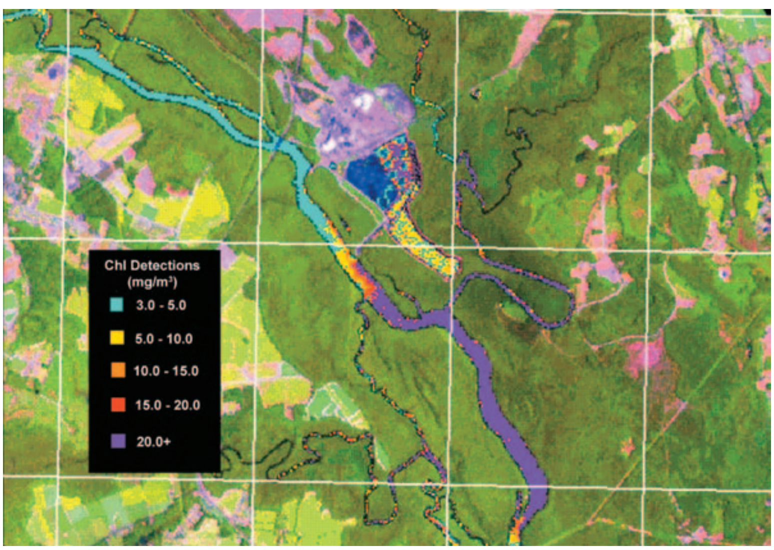

Plate 3. The effects of an industrial site as seen in the AVIRIS-derived chlorophyll thematic map. Outflow from the site appears to cause a dramatic increase in chlorophyll concentration.

within 1 percent of the image-derived values. Others agreed to a lesser extent, depending on the time of sampling and concentration gradients, among other factors.

Impact of Haze and Clouds

There were several locations within the image where low-level clouds/haze crossed the river. At some of these locations where the clouds/haze were optically thick, the software was unable to derive the water quality parameters. No output was reported for those pixels. The spatial patterns of the derived water quality parameters indicated that pixels close to the thick clouds/haze may also have been adversely affected. Areas of thin haze seemed to have little or no apparent impact on accuracy, however, as evidenced by the agreement between the image-derived and field-derived concentrations within and outside of the thin haze occurrences.

Statistical Comparison Conclusions

The statistical correlation analysis was able to provide a quantitative accuracy assessment of the Chl results, but field sampling was inadequate to assess DOC and SM results. The strong correlation between the field and AVIRIS measurements of Chl indicates that AVIRIS has the ability to directly measure Chl. The accuracy of the hyperspectral SM, DOC, and turbidity measurements remains uncertain, however.

Generation of Image Maps of Chl, SM, and DOC

Each pixel in the AVIRIS images was processed independently by the algorithms to produce a measure of Chl, SM, DOC, and turbidity. Separate image output planes for each set of results were generated and can be displayed on the image or by themselves. The measured concentrations were grouped into bins, which were then assigned separate colors for presentation. Imagery-derived thematic maps for Chl, SM, and DOC were generated and are displayed in Plate 2. The spatial distributions of these three water quality parameters are complex and show different large scale patterns of variability. Concentrations are not evenly distributed throughout the river. Steep concentration gradients exist in some areas and large expanses of homogeneous concentrations exist in other areas. Spatial patterns over the entire water surface are revealed which cannot be obtained from limited field sampling.

The Chl map, for example, shows distinct, well defined areas of high and low concentrations. Localized pockets of high Chl exist with sharp concentration gradients. These local areas of high Chl can be important relative to algae blooms if Chl is produced in these areas (as opposed to being transported there). The SM and DOC thematic maps vary in a more uniform and consistent way than do the Chl maps. Only gradual changes in concentration were observed. A general pattern of low to high DOC exists from the left to the right side of the image.

The thematic maps are useful for multiple purposes. One use is for identifying optimal locations for field sampling. This permits more cost-effective and representative field sampling. Sampling can be directed to areas of anomalous conditions, minimum and maximum concentration areas, and along environmental gradients, and can be minimized in large homogeneous areas. The patterns of spatial variability in the maps indicate how field sampling in systematic locations down and across the river (as has been done historically) can provide data that are unrepresentative of many water quality patterns.

Plate 3 shows a location where Chl concentrations increase suddenly in the AVIRIS-derived image, at a specific point on the river. This point appears to be where the outflow pipe from an industrial site enters the river. This pattern of dramatic change cannot be observed visually in the raw AVIRIS imagery. This is an example of how point sources affecting water quality can be identified over large areas. Field sampling could be performed to confirm the remotely sensed measurements.

Other examples were observed where patterns of Chl, SM, or DOC may be explained by land-use patterns in the watershed or close to the riverbank. Land-use patterns such as agriculture, pervious surfaces, and urbanization can be interpreted from the AVIRIS imagery to aid in the analysis of their impact on water quality. At one location, high Chl concentrations occur downstream and around a subdivision with golf courses built immediately adjacent to the river. It is suspected that fertilizer has been used heavily on the golf courses and lawns and has been washed directly into the river, causing algae growth. The thematic maps can be used in a GIS to study the relationships between land use in a drainage basin (derived from the imagery) and the water quality of rivers draining the basin.

Algae Production Potential Index (APPI) Modeling and Thematic Map

Attempts were made to identify additional water quality parameters and to combine water quality measurements to model and predict conditions leading to harmful algae blooms. Chemical and geochemical analyses of the field measurements were conducted to understand the processes taking place in the river. Statistical correlation and principle component analyses were

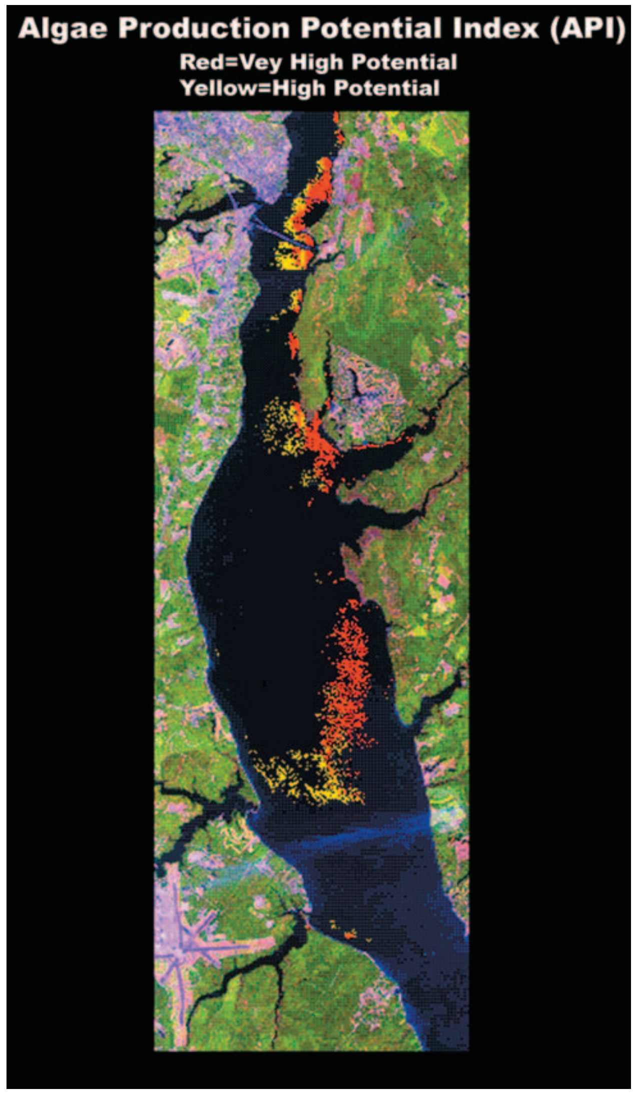

Plate 4. AVIRIS-derived thematic map of the Algae Production Potential Index (APPI).

conducted to identify field parameters correlated with Chl, SM, and DOC. The goal was to see if Chl, SM, or DOC could be used as surrogate measures for other parameters. Details of the analysis will be presented in a separate paper. One observed association was phosphorus compounds with SM. Phosphorus compounds frequently enter the system attached to soil and SM frequently originate from soil. Most other associations were insignificant.

Areas with high Chl concentration represent areas having high phytoplankton concentration. Algae can be produced in, or transported to, these areas. Areas high in both Chl and DOC are more likely to be algae primary production areas, rather than accumulation areas (see discussion by Bukata *et al.*, 1995, pp. 123–123). This is particularly true in fertile waters. In contrast, in nutrient-poor waters DOC is also produced, but it is partially re-assimilated by the photoplankton. DOC is also produced in accumulation zones, but the production rate is typically too low to produce a measurable correlation of Chl and DOC in flowing waters.

Algae production areas also require phosphorus compound input. Indeed, the geochemical analyses indicated that the phosphorus concentration was depressed in samples that otherwise indicated that primary production was occurring. This suggested that algae production might have been phosphorus limited. It was found that phosphorus correlated with SM, which is consistent with expected bonding to soil particles in runoff from fertilized areas. It was deduced that the potential for algae primary production can be predicted and mapped using the spectral imagery by first adding the Chl and DOC image results and identifying areas with combined values greater than a determined threshold. To ensure that these areas were not overly weighted by DOC, the combined high-Chl/high-DOC image results were combined with those of high Chl. Finally, the additional union with high SM (phosphorus compound surrogate) was created.

A GIS model was generated to identify image pixels with high Chl, high DOC, and high SM. The results yielded the thematic map of Algae Production Potential Index (APPI), shown in Plate 4. The APPI map indicates areas of high algae primary production potential at the time of the image collection (20 July 1999, at 10:25 AM). Red indicates "high" production potential areas and yellow indicates "moderate" production potential areas. These may be considered algae bloom "hot spots." The APPI values are qualitative and unit-less for relative comparison rather than quantitative assessment.

The AVIRIS imagery was acquired on a sunny July day. The North Carolina Neuse River Estuary Modeling and Monitoring Program (MODMON, 2001) reports regular occurrences of algae blooms, leading to hypoxic and anoxic conditions, in these segments of the river under sunny conditions in July. The areas of high APPI values are the same size and shape, and are in similar locations to other historic algae blooms reported in the Neuse. It is therefore possible that these high APPI zones correspond to actual or impending blooms. Field verification is needed to validate the APPI results. This will be the focus of future research efforts. Relations between these zones and fish kills, and between point and non-point sources of pollution, are also the subject of a future paper.

The APPI map is an example of how hyperspectral water quality measurements can be used to model and map features associated with higher order ecological processes in a water body or conditions that cannot be directly measured. Several key water parameters were measured directly. One was measured by a surrogate. The parameters were combined based on known relationships and sound phenomenological reasoning, and the results produced information that can only be obtained through modeling. The model makes assumptions and needs to be field verified and validated, but it illustrates how water quality conditions, which cannot be directly measured, can be inferred. When combined and refined with field measurements, weather data, and circulation rates and directions, APPI could be used as a tool to predict fish kills and reduce human health hazards.

Band Averaging to Reduce Noise

Signal-to-noise ratio (SNR) is frequently lower in the shorter wavelength hyperspectral bands over water bodies. Reflectance from a water surface is typically very low, except when dominated by glint or excessive suspended minerals. If noise is significant, the signal from the water can be obscured. Although reasonable SNRs are achievable in the green and longer wavelength regions with many sensors, the blue bands typically have lower SNR, due to detector sensitivity limitations. For deep waters with low suspended mineral concentrations, low signal strengths can introduce noise that affect water quality measurements.

In this project, band averaging was used to increase the SNR in spectral regions critical for water quality analysis. Adjacent bands were averaged to represent the TM band ranges. Noise that is uncommon to each individual band is reduced with this process. Noise reduction was visually apparent as reduced speckling in the averaged bands when displayed.

Even though the TM-equivalent AVIRIS bands were used for most analyses, tests were conducted to determine whether individual AVIRIS bands or the averaged bands produced higher correlations with the field data. Also, the optimal number of bands for averaging was assessed. Results indicate that, in this data set, averaging five bands produced improved results over averaging three bands, both of which were better than using single bands.

These results indicate that noise exists in the AVIRIS blue-, green-, and red-band imagery of dark water bodies, and it limits the extraction of water quality information. Band averaging was a feasible approach for this application because only 21 AVIRIS bands (averaged into three TM-equivalent bands) were used. For other applications, such as spectral signature matching, band averaging may not be appropriate.

Conclusions

The Neuse River is an optically complex water body with highly dynamic circulation and flow. AVIRIS hyperspectral data were used to measure and map the concentration of suspended chlorophyll (Chl), suspended minerals (SM), colored dissolved organic carbon (DOC), and turbidity in the surface waters of the Neuse River Estuary, North Carolina. The statistical correlation analysis provided a quantitative accuracy assessment of the hyperspectral Chl, SM, and DOC measurements. A strong correlation between the field and AVIRIS measurements of Chl ($r = 0.84$) was observed. The SM and DOC results were not directly assessed for accuracy due to problems in the field sampling methodology. A direct accuracy assessment of these parameters needs to be addressed in a follow-on study.

Imagery-derived thematic maps for Chl, SM, and DOC were generated. These maps revealed complex, large-scale patterns of spatial variability that could not be feasibly obtained from traditional field sampling. The thematic maps can be used to identify point and non-point sources of pollution. Some point sources of water quality disturbance, such as an industrial site outflow pipe, can be identified directly from the water quality anomalies in the maps. Visual inspection indicates relationships exist between Chl concentrations and land-cover types known to contain potential non-point source pollutants. For example, high Chl concentrations were observed near tributaries draining agricultural areas and near golf course and housing developments with turf extending the banks of the river (potential sources of fertilizer runoff). Non-point sources such as agriculture, livestock farming, and impervious surfaces can be classified in the imagery and related to the water quality measurements through GIS modeling.

The maps can also be used to identify more cost-effective and representative locations for expensive and time-consuming field sampling. Sampling could be directed to areas of anomalous conditions, minimum and maximum concentration areas, and along environmental gradients, and could be minimized in large homogeneous areas. The spatial patterns in the maps indicate how field sampling in systematic locations down and across the river (as has been done historically) could provide data that are unrepresentative of many water quality patterns.

The APPI map is an example of how water quality measurements from spectral imagery can be used to model and map higher order ecological processes in a waterbody or conditions that cannot be directly field-sampled. Two key water composition parameters were measured directly (Chl and DOC); one was measured by a surrogate (SM for phosphorus compounds). The parameters were combined based on known ecological relationships, and a map was produced depicting areas that had potential for algae primary production. These sites could be algae bloom "hot spots." The model illustrates how water quality parameters or conditions that cannot be directly measured can be estimated. The APPI map, together with the Chl thematic map and the raw hyperspectral imagery (for land-use/land-cover analysis), can be used by water resource managers to understand large scale dynamics of water chemistry and hydrologic flow patterns of algae plumes. When enhanced with weather data, flow rates and directions, and validated with field measurements, APPI could be used as a tool to predict and prevent fish kills and human health hazards.

References

Bukata, R.P., J.H. Jerome, K.Y. Kondratyev, and D.V. Pozdnyakov, 1995. *Optical Properties and Remote Sensing of Inland and Coastal Waters*, CRC Press, Boca Raton, Florida, 362 p.

Copeland, B.J., and J. Gray, 1989. *Albemarle-Pamlico Estuarine System: Preliminary Technical Analysis of Status and Trends*, Albemarle-Pamilco Study Report 89-13A, North Carolina Department of Environmental Health and Natural Resources, Raleigh, North Carolina.

Dekker, A.G., H.J. Hoogenboom, L.M. Goddijn, and T.J. Malthus, 1994. The relationship between spectral reflectance, absorption and backscattering for four inland water types, *Proceedings*, *Sixth International Symposium on Physical Measurements and Signatures in Remote Sensing*, 17–21 January, Val d'Isere, France (CNES), pp. 245–252.

Dekker, A.G., and H.J. Hoogenboom, 1996. Predictive modelling of AVIRIS performance over inland waters, *Summaries of the Sixth Annual JPL Airborne Earth Science Workshop*, 04–08 March, Amsterdam, The Netherlands (JPL Publication 96-4), 1:83–92.

EPA, 1996. *The National Water Quality Inventory Report to Congress*, *1996*, Office of Water Quality, U.S. Environmental Protection Agency, Washington, D.C., 200 p.

Goetz, A.F.H., G. Vane, J.E. Solomon, and B.N. Rock, 1985. Imaging spectrometry for Earth remote sensing, *Science*, 228:1147–1153.

Gordon, H.R., and A. Morel, 1983. Remote assessment of ocean color for interpretation of satellite visible imagery: A review, *Lecture Notes on Coastal and Estuarine Studies* (M. Bowman, editor), Springer-Verlag, New York, N.Y., p. 114.

Holyer, R.J., and J.C. Sandidge, 1996. Coastal bathymetry from hyperspectral data, *Summaries of the Sixth Annual JPL Airborne Earth Science Workshop*, 04–08 March, Stennis Space Center, Mississippi (JPL Publication 96-4), p. 147.

Huguenin, R.L., M.H. Wang, R. Biehl, S. Stoodley, and J.N. Rogers, 2004. Automated subpixel photobathymetrty and water quality mapping, *Photogrammetric Engineering & Remote Sensing*, 70(1):111–123.

Jensen, J.R., B. Kjerfve, E.W. Ramsey III, K.E. Magill, C. Medeiros, and J.E. Sneed, 1989. Remote sensing and numerical modeling of suspended sediment in Laguna de Terminos, Campeche, Mexico, *Remote Sensing of Environment*, 28:33–44.

Karaska, M., and R.L. Huguenin, 2002. *NASA EOCAP Hyperspectral Imagery and Water Quality Assessment Milestone 12: Final Report*, internal document, NASA Stennis Space Center, Mississippi, 43 p.

Khorram, S., and H.M. Cheshire, 1985. Remote sensing of water quality in the Neuse River Estuary, North Carolina, *Photogrammetric Engineering & Remote Sensing*, 51(3):329–341.

MODMON, 2001. The Neuse River Estuary MODeling and MONitoring Project, North Carolina Department of Environmental and Natural Resources and the University of North Carolina Water Resource Research Institute, URL: http://www.marine.unc.edu/neuse/modmon/publications/summary_2001.pdf, last accessed 24 October 2003.

Paerl, H.W., M.A. Mallin, C.A. Donahue, M. Go, and B.L. Peierls, 1995. *Nitrogen Loading Sources and Eutrophication of the Neuse River Estuary*, *North*, *Carolina: Direct and Indirect Roles of Atmospheric Deposition*, Report No. 95-291, Water Resources Research Institute, University of North Carolina, Raleigh, North Carolina, 199.

Paerl, H.W., J.L. Pinckney, J.M. Fear, and B.L. Peierls, 1998. Ecosystem responses to internal and watershed organic matter loading: Consequences for hypoxia in the eutrophying Neuse River Estuary, North Carolina, US, *Marine Ecology Progress Series*, 166: 17–25.

Pinckney, J.L., M.B. Harrington, and K.E. Howe, 1988. Annual cycles of phytoplankton community-structure and bloom dynamics in the Neuse River Estuary, North Carolina, *Marine Biology*, 131: 371–381.

Ramsey, E.W., and J.R. Jensen, 1990. Derivation of water volume reflectances from airborne MSS data using in situ water volume reflectances and a combined optimization technique & radiative transfer model, *International Journal of Remote Sensing*, 11(6):979–998.

Ramsey, E.W., J.R. Jensen, H. Mackey, and J. Gladden, 1993. Remote sensing of water quality in active to inactive cooling water reservoirs, *International Journal of Remote Sensing*, 13(18):3465–3488.

Richardson, L.L., and F.A. Kruse, 1999. Identification and classification of mixed phytoplankton assemblages using AVIRIS image-derived spectra, *Summaries of the Eighth JPL Airborne Earth Science Workshop*, 09–11 February, Pasadena, California (JPL Publication 99-17), pp. 339–347.

Woodruff, D.L., R.P. Stumpf, J.A. Scope, and H.W. Paerl, 1999. Remote estimation of water clarity in optically complex estuarine waters, *Remote Sensing of Environment*, 68:41–52.

(Received 30 May 2002; accepted 31 January 2003)